Environmental Earth Sciences (2023) 82:569
https://doi.org/10.1007/s12665-023-11225-2

ORIGINAL ARTICLE

Assessments of land subsidence in Tehran metropolitan, Iran, using Sentinel-1A InSAR

Aydin Moradi[1] · Somayeh Emadodin[2] · Ali Beitollahi[3] · Hadi Abdolazimi[3,4] · Babak Ghods[5]

Received: 5 November 2022 / Accepted: 7 October 2023 / Published online: 15 November 2023

Abstract

The metropolis of Tehran, the capital and the largest city of Iran, has been affected by the phenomenon of land subsidence in the past years. Up to now, no comprehensive study has been presented on land subsidence in the Tehran metropolis. This study addresses this shortcoming through a comprehensive investigation of surface and sub-surface factors that affect the subsidence and investigates the mechanism of subsidence development in Tehran. Land surface studies involve assessing the subsidence rate by utilizing InSAR technology, tracking the urban development of the city through time, and investigating geomorphological features like the alluvial fans landforms and surface drainage. Sub-surface studies include groundwater and geotechnical assessments. The evaluations indicate that the combinations of soils with a high percentage of fine grains and the drop in the underground water level are the major drivers of subsidence in the south of Tehran. The results of the study showed that the highest rate of land subsidence is 217 mm/year and has happened in the southwest of Tehran city. Districts 10, 11, 16, 17, 18, 19, and 20, which comprise about 26% of Tehran's population (about 2.3 million people in 2016), are affected by subsidence. According to the results obtained from the geomorphological studies, these areas are located at the end of the alluvial fan of Kan and Chitgar (south and southwest of Tehran). The paper also focuses on the sharp northward growth of the subsidence zone in the northeast corner of Tehran's subsidence zone. From investigations, it is concluded that changes in four river courses (which lead to a drop in the underground water level) in conjunction with fine grain soil of this area are (probably) the major factors that have played a role in the northward growth of the subsidence zone at the northeastern corner. The paper also identifies the most vulnerable urban districts affected by the subsidence as well as some major infrastructures exposed to subsidence hazards.

Keywords Land subsidence · Tehran · InSAR · Geomorphology · Geotechnical studies · Urban decay

Introduction

The phenomenon of land subsidence involves the collapse or sinking of the earth's surface, which can also have a slight horizontal displacement vector. This movement is not limited in terms of intensity, extent, and size of the involved areas (Ge et al. 2007). The phenomenon of land subsidence can damage surface and sub-surface structures and cause significant financial, social, and environmental losses (Sun et al. 1999; Sneed et al. 2003; Ge et al. 2007; Teatini et al. 2006; Galloway and Burbey 2011Yastika et al. 2019). Several factors may cause land subsidence. Earthquakes (Shenan and Hamilton 2006), dissolution (Zidane et al 2014), freezing (Galloway and Burbey 2011), and compaction of sediments (Kooi and Veries 1998), lava outflows (Chaussard 2016), or human operations, such as oil or groundwater

✉ Somayeh Emadodin
s.emadodin@gu.ac.ir

1 Shahid Beheshti University, Tehran, Iran

2 Department of Geography, Faculty of Humanities and Social Sciences, Golestan University, Gorgan, Iran

3 Scientific Board of Engineering Seismology and Risk Department, Road, Housing and Urban Development Research Center (BHRC), Tehran, Iran

4 Department of Remote Sensing and GIS, Shiraz Branch, Islamic Azad University, Shiraz, Iran

5 Civil Engineering Department, Sharif University of Technology, Tehran, Iran

extraction (Kearns et al 2015), are some of the factors that play a major role in land subsidence.

In recent decades, rapid population growth along with urban, industrial, and agricultural development has led to an increase in water consumption around the world. Consequently, harvest at underground water tables has increased in many populated cities, especially in countries with arid and semiarid climates. In turn, this increase in underground water harvest can lead to land subsidence which causes significant social, economic, and environmental problems.

Examples of subsidence due to excessive groundwater pumping can be found around the world for example in Turkey (Yesilmaden et al. 2021), Nairobi Aquifer System (NAS) in Kenya (Nyakundi et al. 2022), eastern China (Li et al. 2023), Parowan Valley, Utah, USA (Li et al. 2023). Different parts of Iran are also dealing with the subsidence phenomenon. Places like Mashad (Motagh et al. 2008), Qom (Rajabi 2018), Esfehan (Goorabi et al. 2020), Shiraz (Karami et al. 2023), and Rafsanjan (Bockstiegel et al. 2023) are a few examples in this regard.

Similar to the aforementioned cases, Tehran has been affected by the subsidence phenomenon since the 1990s (Amighpey et al 2006). It seems the sprawl of Tehran, including the construction of buildings, the development of important arteries, and also the subway system, has had a significant role in aggravating subsidence; therefore, it is needed to study and continuously track the land subsidence in this metropolitan, (Motagh et al. 2008; Dehghani et al. 2013; Esmaeili and Motagh 2016; Esmaeili et al. 2017; Haghshenas Haghighi and Motagh 2019; Mahmoudpour et al. 2016). Due to its high sensitivity, many studies have been conducted on land subsidence in the metropolis of Tehran (Motagh et al. 2008; Pishro et al. 2016; Pirouzi and Eslami 2017; Ranjbar and Ehteshami et al. 2019; Chatrsimab et al. 2020; Yousefi and Talebeydokhti 2021).

Motagh et al. (2008) were among the first researchers who investigated the subsidence of Tehran. By combining water-level data with satellite radar observations, they showed that the drop in groundwater levels is associated with land-surface deformation on local and regional scales. In another study, Pishro et al. (2016) modeled the land subsidence in Tehran using an artificial neural network. They used nine important factors (e.g., the downfall of groundwater, the thickness of the clay, depth of groundwater, annual discharge, etc.) to study the subsidence. They concluded that the areas with the underground water drop and agricultural land uses are the most susceptible areas to land subsidence occurrence. In a more recent study, Rajabi Baniani et al. (2021) used the standard persistent scatterer interferometry (PSI) method to assess the subsidence rate in Tehran. They estimated that the maximum loss of elevation for 2018–2019 is about 11.7 cm/year. They also found that groundwater withdrawal is an important driving mechanism of subsidence, but the variation in soil type also plays an important role. However, they did not further investigate this subject. Another recent work in this regard was done by Yousefi and Talebeydokhti in 2021 (Yousefi and Talebeydokhti 2021). In that study, they used synthetic aperture radar interferometry (InSAR) with two radar images to assess the subsidence. Their results indicate a low correlation between subsidence and groundwater exploitation. However, they also suggest a direct relationship between subsidence and aquitard thickness (although this conclusion may seem somewhat counterintuitive, as a drop in groundwater levels is generally considered one of the main factors contributing to subsidence).

As can be seen, most of the studies in Tehran focus only on assessing the land subsidence rate due to underground water loss or numerical modeling of the subsidence (to predict the future of this phenomenon). However, in terms of comprehensive evaluation and investigation of the subsidence phenomenon, especially the investigation of sediment size distribution at different depths, the amount of resistance and compressibility of sediments, and the role of geomorphology landforms, less attention has been paid. Therefore, most of the studies do not provide a thorough explanation of the reason behind this phenomenon in Tehran. Also, the investigation of urban areas exposed to this phenomenon has not been done rigorously in the studies. This research tries to address this scholarly gap through a comprehensive investigation of land subsidence in Tehran considering all the aforementioned determinants. In particular, the paper is focused on the assessment of the subsidence rate in the Tehran metropolitan and a comprehensive investigation of its reasons and addresses the following concerns:

i. What is the spatial and temporal distribution of subsidence in this city?
ii. Which parameters play the most important roles in the spatial and temporal distribution of subsidence rate and how?

To address the first concern, Interferometric Synthetic Aperture Radar (InSAR) technology is utilized to determine the spatial and temporal distribution of subsidence in the city. To address the second concern, the study is focused on two parts: land-surface studies and sub-surface studies. In addition to investigating the subsidence rate, land-surface studies involve tracking the urban development of the city and investigating some geomorphological features like the alluvial fans landforms and surface drainage. Sub-surface studies include groundwater and geotechnical assessments.

By examining these land-surface and sub-surface features, the major factors that contribute to the subsidence

in the southern part of Tehran are investigated and the mechanism of subsidence development in Tehran is discussed. In particular, the paper focuses on the northward growth of the subsidence at the northeast corner of the subsidence zone (in the south of Tehran). Studying the northeast corner of the subsidence zone is significantly important as it covers populated (and also structurally vulnerable) districts of Tehran (i.e., District 10 with over 300,000 population). As will be shown in the rest of the paper, from the land-surface studies and sub-surface investigations (like geotechnical investigation and SPT tests), it is concluded that a complex effect of some anthropogenic actions (like examining the temporal evolution of four river courses in Tehran) in conjunction with soil grading, are (probably) the major factors that have played a role in the Theran's subsidence and the growth of the subsidence zone at the northeastern corner. Based on the paper's findings, some suggestions are also made to mitigate the subsidence growth in this area. Moreover, other residential regions of Tehran in the major subsidence-prone zones are identified in this study. Therefore, the documentation of this research can be used in the hazard management of subsidence, especially in the mitigation phase.

In the rest of this paper, the description and explanation of information related to the study area are discussed first (in the section "Study area"). Next, in the section "Methodology", methodologies for land-surface and sub-surface studies are presented in more detail. Then, in the section "Results and discussion", the data analysis result, including the spatial analysis of the subsidence phenomenon, is presented and discussed. Furthermore, major influencing factors on the phenomenon are identified and presented in this section. A summary discussion about the mechanism of subsidence development in Tehran is presented at the end of this section. The section "Urban studies: evaluation of residential density, urban development, and urban decay affected by land subsidence" presents the most vulnerable urban districts affected by the subsidence as well as some major infrastructures exposed to subsidence. Moreover, some suggestions on necessary actions regarding mitigating the subsidence will be expressed in the section "Urban studies: evaluation of residential density, urban development, and urban decay affected by land subsidence". Finally, the general summary and conclusion are presented.

Study area

The city of Tehran (Fig. 1), which extends almost from east to west along the southern slope of the Alborz mountain range, is located in the northern part of the plain with an average height of 1300 m above the average sea level. The city of Tehran is constructed on the alluvial deposits of the Quaternary period and the age of the sediments is at most 5 million years. The alluviums originated from the floods of the late Cenozoic period and at the same time as the elevation of the Alborz mountains, they were deposited in the lowlands. Tehran, as the capital of Iran, has experienced huge population growth over the past 40 years. Large-scale migration is the main reason for the unprecedented growth of population in Tehran province, which now hosts almost 13 million people compared to less than 6 million in 1979.

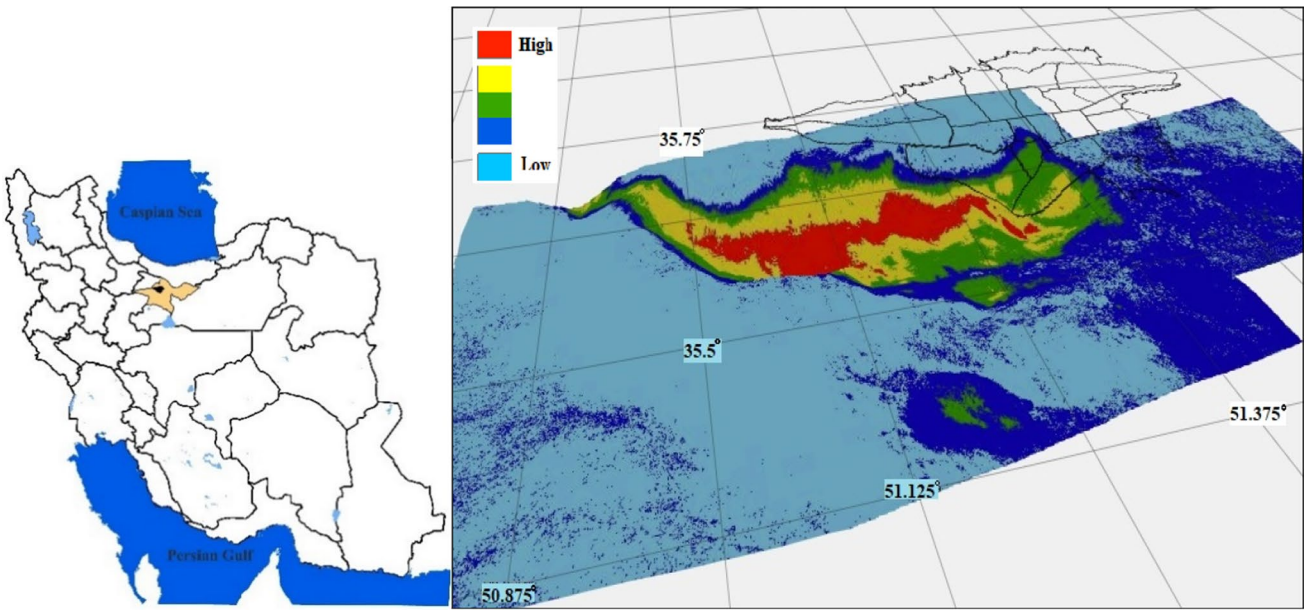

Fig. 1 The geographical position of study area

Several dams were built in the 1960s along the main course of rivers in the region to divert surface water for agricultural, urban, and industrial use. However, these sources do not meet the water needs of the region. Currently, underground water is the main source of water for irrigation of agriculture and industries in Greater Tehran (Haghshenas Haghighi and Motagh 2019). As was mentioned in the introduction, severe ground subsidence is experienced in the Tehran metropolitan.

Methodology

In the current research, the study has been categorized into different sections that are shown in a flowchart of Fig. 2. The surface studies include the remote-sensing operations: estimation of the subsidence rate and the determination of the subsidence pattern in the Tehran metropolitan using radar interferometry; and also geomorphological investigations: studying of alluvial fans, verification of the landforms by aerial photograph, sampling of the ground surface, and the sedimentology. As was mentioned, urban development was also examined in the surface studies. The sub-surface studies including groundwater and geotechnical analysis (preparation of fine, sand, and gravel distribution map and investigation of SPT) were also done. The selected surface and sub-surface features were chosen by considering the studies that have been done on this phenomenon and identifying the major parameters that could affect the subsidence. Although the main affecting parameter on subsidence is the drop of underground water, as will be shown, other parameters influence the subsidence significantly (e.g., geotechnical parameters). Furthermore, to have a proper understanding of the subsidence phenomenon, it is important to investigate what natural or anthropogenic factors affect the drop in water levels in a region. By investigating the selected surface and sub-surface parameters in conjunction with the generated subsidence maps, the authors have provided their interpretation of the complex mechanism and causes of subsidence in Tehran and the reasons for the growth of the subsidence zone in the northeast corner. In the rest of this section, the gathered data and information, the procedure used for the analysis of the data, and the type of results that are created in the surface and sub-surface analysis are presented. However, the presentation of the results and discussion on them are done in the sections "Results and discussion" and "Urban studies: evaluation of residential density, urban development, and urban decay affected by land subsidence".

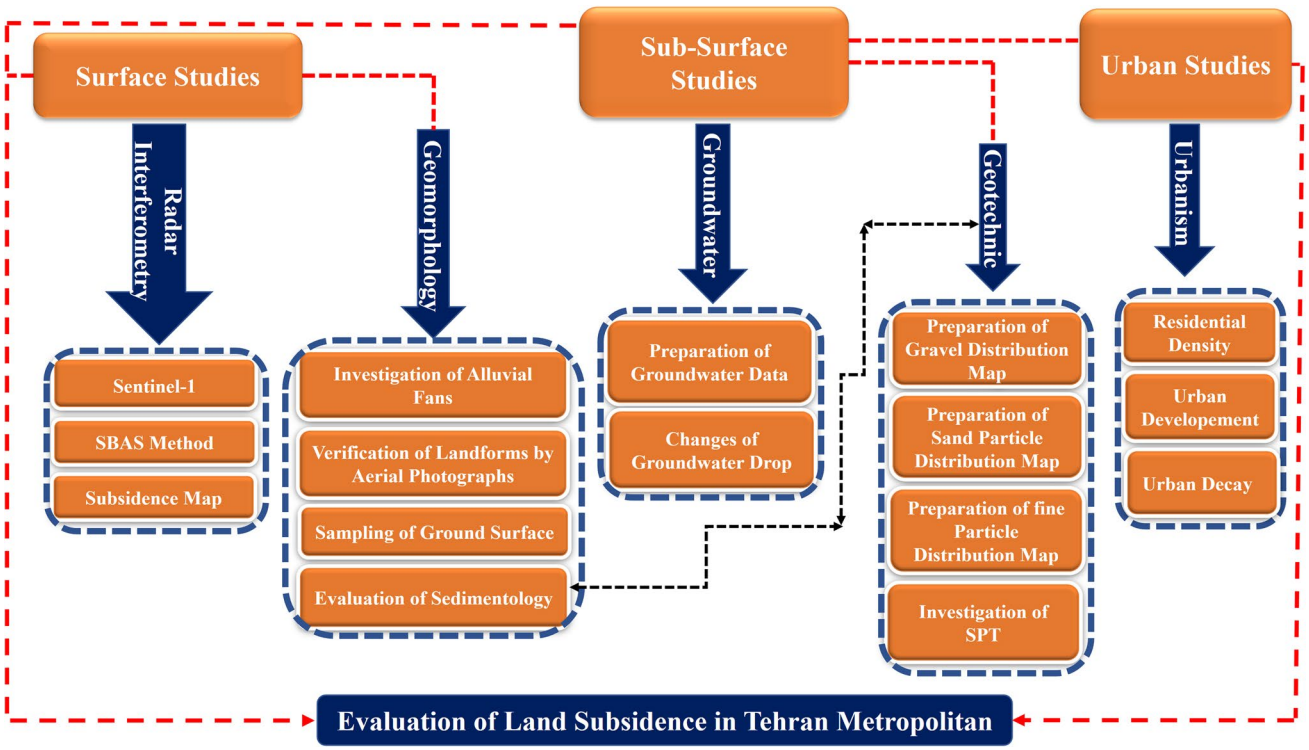

Fig. 2 The trend of this research

First stage: land-surface studies

First step: determining the rate and pattern of land subsidence (radar interferometry)

The first step in assessing the subsidence at any region is to provide the subsidence maps. As shown in Fig. 2, in the first step of the land-surface studies, Sentinel-1 images of slc type are used to prepare the subsidence map. 13 images are selected along with orbital information in a period of 2 years (2017–2019), and then, the SBAS method (proposed by Berardino in 2002 (Berardino et al. 2002) is utilized to prepare a subsidence map. The more detailed steps of the procedure are presented in the following.

The mathematical principles of radar interferometry are such that SAR images contain two real and imaginary parts, which are written as Eq. 1 (Strozzi et al. 2002)

$$y = |a|e^{i\varphi}. \tag{1}$$

In this equation, $|a|$, φ, and i are the amplitude, phase, and imaginary unit, respectively. The phase of interferometry is calculated from the complex multiplication of the main image in the different conjugates of the secondary image according to Eq. 2

$$y_m\bar{y}_s = |a_m|e^{i\varphi_m}|a_s|e^{i\varphi_s} = |a_m||a_s|e^{(\varphi_m-\varphi_s)}. \tag{2}$$

In this equation, 'm' is the master image and 's' indicates the slave image. After calculating the phase difference of two SAR images, an interferogram is generated. Figure 3 shows the graph related to the formation of interferograms. In this figure, the vertical axis is the spatial baseline and the horizontal axis is the time baseline. The lines that connect the images indicate the formed interferograms. In the SBAS method, pairs of images whose baseline is lower than the critical value and whose temporal baseline is as minimal as possible are used. In this way, only interferograms that have proper coherence are formed. The main components in the interferogram phase according to Eq. 3 are

$$\varphi_{\text{int}} = \varphi_m - \varphi_{ms} = \varphi_{\text{def}} + \varphi_{\text{topo}} + \varphi_{\text{flat}} + \varepsilon_{\text{error}}. \tag{3}$$

According to Eq. 3, the phase component φ_{def} is the earth's surface deformation, φ_{topo} is the phase due to topography, φ_{flat} is the phase due to the flatness of the earth, and $\varepsilon_{\text{error}}$ is the disturbing phase components including the atmospheric phase, the orbital ramps, and the residual phase related to noise in the interferogram. After forming interferograms, a grid of images is created and different phase factors, such as atmosphere, topography, orbital errors, and flat earth, are removed. To eliminate the effect of topography, an interferogram from the DEM of the studied area was simulated in the geometry of the radar and subtracted from the interferograms. At this stage, ASTER DEM was used to check the time-series and remove the effect of the orbital error from the interferograms. Next, an image was selected as the original date and the changes of other images were measured relative to it. The interferograms were subjected to least-squares analysis to calculate the amount of displacement of each pixel (Dang et al. 2014). After obtaining the displacement phase for each time interval, the amount of displacement per pixel of the interferograms was obtained with the coefficient in the estimated phase. In this way, the time-series was selected for each of the pixels (Fig. 4). Finally, the average displacement speed in each pixel and in the desired time interval was obtained by fitting each time-series. In this way, the average displacement per year was obtained.

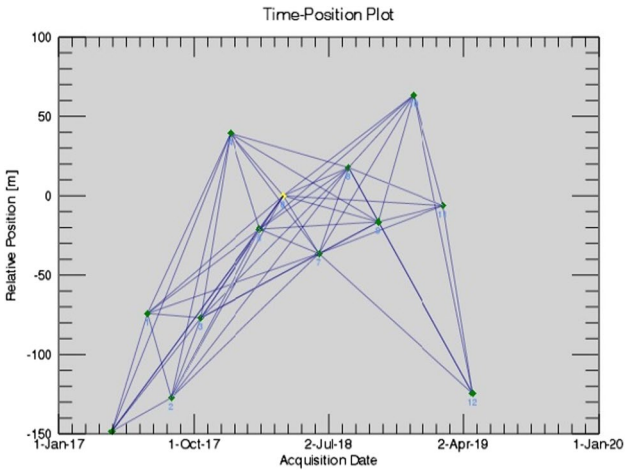

Fig. 3 The graph of formed interferograms

Second step: alluvial fans' landforms, surface drainage, urban development, and sedimentology

Geomorphological investigations like assessing the alluvial fan landforms, main waterways (and their natural or man-made changes through time), and urban development could provide insights into the influencing parameters on subsidence in an area. For example, by studying the alluvial fans along with the subsidence maps, a general view of the relationship between the soil grading and subsidence is at hand. Moreover, comparing the old city texture and new urban texture provides information on the anthropogenic factors that have influenced the subsidence.

In this regard, first, the 1:55,000 aerial photos related to the year 1956 were scanned, and then, the photos were mosaicked and geo-referenced (Fig. 5). New information on urban areas and main waterways was also obtained from the Road and Urban Development Research Center, which was further compared with old aerial photographs. Aerial photos indicate that the city of Tehran has had more than 22 times in physical development which indicates high anthropogenic

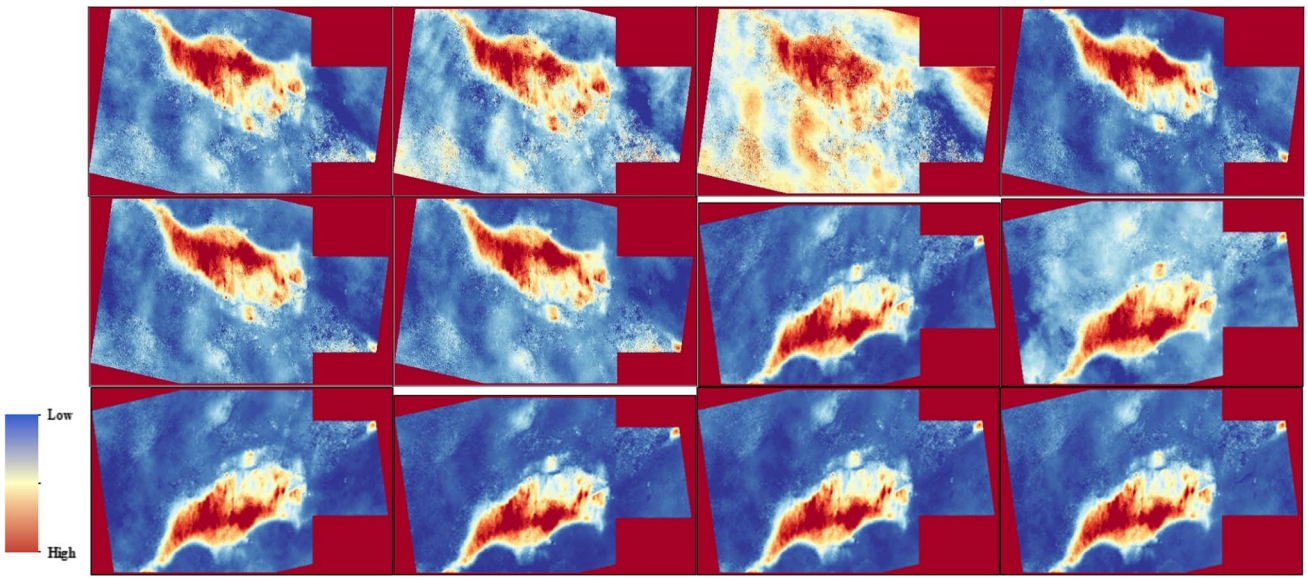

Fig. 4 The pattern of ground displacement changes in the period from 29.05.2017 to 20.04.2019. In this study, the images were selected with a time interval of 2 months, which includes a total of 13 images, and 12 images of the earth's surface displacement were obtained, which have the same pattern

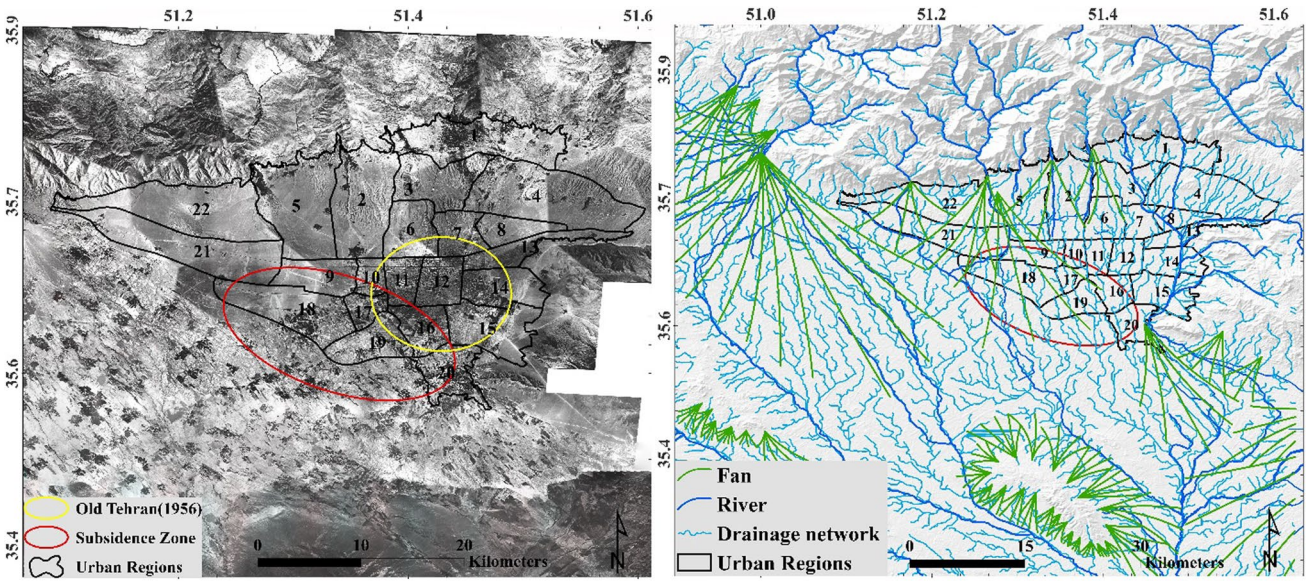

Fig. 5 Aerial image of the study area in 1956 and drainage network map and alluvial fans

effects on the environment. Then, alluvial fan landforms were drawn manually (Fig. 5). The result of this section includes the map of alluvial fan landforms, main waterways, old city texture, and new urban texture.

In the urban studies, information related to residential density and the urban decay of each of the 22 urban districts was extracted from the statistical yearbook of Iran's statistical center (Table 1). The areas that were in the land subsidence zone were identified. Physical changes in 1956 and 2017 were also investigated. Finally, sedimentology studies were conducted at this stage to provide an overview of Tehran's soil properties and grading. The detail of the sedimentology studies is presented in the next subsection.

Investigation of sedimentology in the study area In this step, taking into account the distribution of the topographic slope (Table 2), the studied area was divided into three northern, middle, and southern areas and sampling was done. There

Table 1 Residential and population information of 22 districts of the Tehran metropolis

District	Area (hectares)	Residential density	Worn texture (hectares)	District	Area (hectares)	Residential density	Worn texture (hectares)
1	4572	35	64	12	1597	47	593
2	4768	48	19	13	1701	56	73
3	2935	40	25	14	2201	74	257
4	6156	47	7	15	3068	62	246
5	5320	57	12	16	1652	54	149
6	2140	38	6	17	822	95	240
7	1536	75	237	18	3807	36	103
8	1322	107	144	19	2053	34	22
9	1948	26	146	20	2074	51	137
10	806	139	146	21	5137	10	7
11	1204	88	352	22	5849	10	5

Table 2 Characteristics of the divided areas in the sedimentology department

Zone name	Slope %	Area (hectares)
Zone no. 1	7	18,333
Zone no. 2	3	16,603
Zone no. 3	1	25,382

were limitations such as the presence of urban elements that led to the loss of alluvial deposits and natural alluvial cones. For this reason, the samples were taken from points such as the walls of waterways, excavations, trenches, and complications that are less disturbed. A total of 37 points were selected for sampling. The northern zone includes 14 points, the middle zone 11 points, and the southern zone 12 points (Fig. 6).

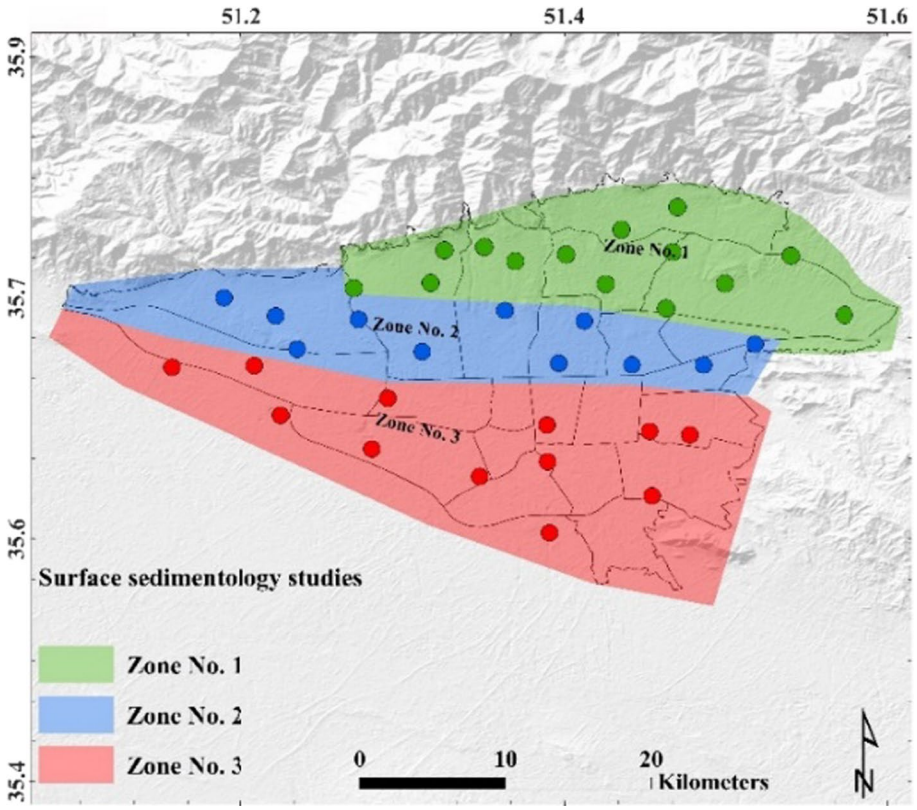

Fig. 6 Location map of sampled points in the sedimentology department

The samples were utilized to study grain size along with roundness, skewness, and spreading of sediments. In particular, after taking samples from the selected points, the samples were sieved using a dry sieve, and their weight percentage was measured in the sizes of gravel, sand, and fine grains of silt and clay. Calipers were used to analyze the shape of grains larger than 30 mm. The large and small diameter of seeds was measured and the average of each sample was used to calculate the form, expansion, sphericity, and roundness. Sphericity according to Eq. 4 was obtained from the second root of the ratio of the smallest diameter of the circle that the seed contains to the largest circular diameter of the seed. (Rodriguez and Edeskar 2013)

$$\text{Riley sphericity} = \sqrt{\frac{\text{Di}}{\text{Dc}}}, \tag{4}$$

Di: Diameters of Inscribed. Dc: Diameters of circumscribed.

Roundness is obtained from Eq. (5), which quantifies the ratio of the sharpest corner of the grain to the radius of the largest circle surrounded by the grain (Dobkins and Folk 1970)

$$P = r/R, \tag{5}$$

P: roundness. *r*: the radius of the sharpest corner of the grain. R*:* the radius of the largest circumference of the circle.

Equation 6 was used to calculate the width ratio

$$W = (a + b)/(2 * c), \tag{6}$$

a: large diameter, *b*: medium diameter, *c*: small diameter, and *w*: width ratio.

The clay particles were measured using the pipette method. To accomplish this step, 10 g of samples that were smaller than 63 µm in size (after being ground and sieved) were poured into a graduated cylinder. Using Stokes' law, the weight of the clay particles was determined from 62.5 to 0.49 µm. The major information obtained from the samples is prepared in the form of graphs and tables which will be explained in the section "Results and discussion".

Second stage: sub-surface studies

First step: groundwater

The groundwater level is the major influencing factor on subsidence and should be investigated properly. To study the latest status of the groundwater level (Table 3) in the study area, the information on 102 piezometric wells for the years 2001 and 2017 was collected from the Tehran Regional Water Organization, and then, these data were analyzed. The groundwater level map in the mountainous areas, north of Tehran, was ignored. Due to the mountainous nature of the northern areas, the groundwater system is in the form of streaks and is in contrast with the southern parts of the city, which are mostly flat plains and have an underground water reservoir. The groundwater map was drawn using 2017 data. Also, the amount of water-level changes in the mentioned years was extracted and prepared as a graph.

Second step: geotechnics

Studies have shown that in addition to the drop in groundwater levels, the soil properties could also affect the subsidence. Therefore, a major part of this research is focused on determining the geotechnical properties at different regions in Tehran city and investigating their association with the subsidence. In this regard, information on the number of 1000 geotechnical boreholes was obtained from the geotechnical bank of the Road, Housing, and Urban Development Research Center. After the investigation of the borehole data, the information from 500 boreholes was used to evaluate the distribution of granulation at different depths. Another parameter used is the evaluation of the standard penetration test (SPT) figures of the area affected by land subsidence.

The statistical data of the distribution of fine grains, sand, and gravel at depths of 5, 10, 15, 20, 25, and 30 m were recorded as a percentage, and then, the interpolation technique (IDW) was used to prepare a grain size zoning map. Using this information, a distribution map of grain size and texture of sediments (in terms of abundance percentage) was drawn at the mentioned depths. Next, from the SPT data of the boreholes, two profiles were prepared in the geographical directions of northeast–southwest and northwest–southeast, and the correlation between SPT and subsidence was investigated as an influencing factor.

Results and discussion

Results of surface studies

Subsidence zone and features

The result of the radar interferometric study in Fig. 7 shows that in the south and southwest parts of Tehran, land subsidence is taking place in an area of more than 700 square kilometers, which also includes parts of the Tehran metropolis. The maximum average land subsidence rate was 217 mm, which is outside of Tehran city (Fig. 7). In the urban areas, the highest average annual land subsidence rate was found in District 18. District 17 has the second order among the 22 districts. Urban districts 10, 11, 16, 17, 18, 19, and 20 are also affected by land subsidence. As can be seen from

Table 3 Groundwater level information in 2011 and 2017

Name	*X*	*y*	2001	2017	Drop rate	Name	*X*	*y*	2001	2017	Drop rate
1	513,715	3,941,962	36.6	36.7	− 0.1	52	507,700	3,942,770	47	53.96	− 6.96
2	519,018	3,943,377	67.3	71.56	− 4.26	53	506,210	3,949,610	111.85	136.24	− 24.39
3	504,514	3,943,943	23.8	30.91	− 7.11	54	534,076	3,934,069	24.7	41.07	− 16.37
4	517,404	3,947,425	53.45	74.18	− 20.73	55	533,925	3,950,992	86.15	82.93	3.22
5	518,996	3,943,371	48	48.16	− 0.16	56	514,208	3,926,533	17.42	18.81	− 1.39
6	510,830	3,931,550	35.4	44.49	− 9.09	57	522,592	3,913,298	66.6	66.98	− 0.38
7	525,599	3,953,214	107.2	113.98	− 6.78	58	535,842	3,952,144	78.9	94.64	− 15.74
8	536,270	3,907,206	44.17	33.71	10.46	59	517,402	3,947,425	43.94	76.23	− 32.29
9	547,592	3,934,518	6.15	15.3	− 9.15	60	514,035	3,946,349	67	71.75	− 4.75
10	537,163	3,938,931	15.5	24.18	− 8.68	61	525,430	3,947,426	113.8	131.7	− 17.9
11	512,350	3,950,650	105.15	114.7	− 9.55	62	547,881	3,953,655	71.15	76.7	− 5.55
12	503,498	3,948,916	127.8	151.54	− 23.74	63	481,730	3,947,280	18.16	22.7	− 4.54
13	537,840	3,904,200	33.66	44.96	− 11.3	64	501,260	3,941,950	17.52	20.6	− 3.08
14	509,686	3,946,700	101.8	109	− 7.2	65	517,847	3,914,140	63.8	44.45	19.35
15	510,460	3,943,700	47.9	56.71	− 8.81	66	526,047	3,956,699	127.6	127.9	− 0.3
16	531,961	3,953,693	103	117	− 14	67	501,430	3,948,770	131.93	138.9	− 6.97
17	544,276	3,947,745	37.4	62	− 24.6	68	522,885	3,955,858	114	122.06	− 8.06
18	528,636	3,942,382	29.5	31.5	− 2	69	493,608	3,951,021	62.1	81.2	− 19.1
19	518,151	3,939,443	42	25.48	16.52	70	534,171	3,926,476	16.5	23.95	− 7.45
20	543,980	3,951,699	68.15	92.02	− 23.87	71	539,320	3,930,137	16.5	16.74	− 0.24
21	520,560	3,952,607	78.75	83.9	− 5.15	72	518,422	3,929,099	32.9	51.78	− 18.88
22	537,783	3,934,559	14.6	26.95	− 12.35	73	553,455	3,928,934	5.7	15.85	− 10.15
23	514,063	3,949,090	75.26	106.7	− 31.44	74	521,655	3,941,180	33	33.78	− 0.78
24	532,659	3,938,078	19.5	32.23	− 12.73	75	547,363	3,954,758	85	92.65	− 7.65
25	545,570	3,929,336	3.6	5.25	− 1.65	76	523,909	3,945,612	91.34	110.93	− 19.59
26	498,216	3,937,180	58.41	64.6	− 6.19	77	512,583	3,922,097	92	105.05	− 13.05
27	509,293	3,926,785	61.55	42.7	18.85	78	549,536	3,954,122	36.6	54.08	− 17.48
28	520,416	3,916,110	84.9	96.95	− 12.05	79	509,180	3,951,000	105.15	150	− 44.85
29	516,628	3,950,951	92.1	109.76	− 17.66	80	509,914	3,950,054	96.61	112.3	− 15.69
30	528,264	3,936,008	20.4	26.69	− 6.29	81	520,050	3,944,060	127.8	150.5	− 22.7
31	544,446	3,928,749	4.75	7.52	− 2.77	82	546,430	3,929,700	1.3	4.4	− 3.1
32	515,244	3,953,368	106.5	128.73	− 22.23	83	537,651	3,929,194	6.1	7.28	− 1.18
33	519,219	3,935,664	32.15	26.33	5.82	84	536,050	3,945,380	12.82	30.9	− 18.08
34	522,282	3,915,215	73.5	150	− 76.5	85	507,029	3,930,983	14.27	16.1	− 1.83
35	520,100	3,917,040	90	96.31	− 6.31	86	530,944	3,928,058	7.75	10.9	− 3.15
36	528,286	3,954,117	136	143.95	− 7.95	87	500,663	3,945,240	100.1	119	− 18.9
37	529,184	3,938,750	28.85	30.91	− 2.06	88	548,283	3,932,198	1.05	3.28	− 2.23
38	487,468	3,949,579	22.85	20.09	2.76	89	551,141	3,926,213	1.8	4.9	− 3.1
39	504,450	3,944,040	22	24.84	− 2.84	90	496,868	3,951,926	116.8	145	− 28.2
40	496,370	3,946,580	91.51	91.33	0.18	91	542,452	3,955,846	124.8	141.08	− 16.28
41	517,622	3,922,355	63.7	73.81	− 10.11	92	522,418	3,937,658	44.3	45.5	− 1.2
42	548,676	3,922,427	11	11.7	− 0.7	93	496,972	3,941,339	11.95	15.32	− 3.37
43	548,653	3,922,470	1.7	3.3	− 1.6	94	540,290	3,946,781	6.18	19.7	− 13.52
44	530,748	3,909,420	35.21	58.48	− 23.27	95	531,042	3,948,913	85.6	101.7	− 16.1
45	533,114	3,940,416	14.94	15.08	− 0.14	96	525,835	3,932,275	11.3	15.01	− 3.71
46	527,365	3,928,412	7.7	17.3	− 9.6	97	526,693	3,914,752	29.49	30.57	− 1.08
47	541,423	3,942,312	14.2	24	− 9.8	98	512,727	3,955,560	61.33	86.9	− 25.57
48	543,104	3,932,935	4.55	11.06	− 6.51	99	501,390	3,953,160	146.9	160.6	− 13.7
49	514,570	3,938,200	48.8	54	− 5.2	100	527,003	3,944,728	78.8	90.73	− 11.93
50	524,769	3,935,564	18.3	25.98	− 7.68	101	503,300	3,935,280	18.5	22.52	− 4.02

Table 3 (continued)

Name	*X*	*y*	2001	2017	Drop rate	Name	*X*	*y*	2001	2017	Drop rate
51	514,035	3,938,959	28.21	29.7	− 1.49	102	492,025	3,948,063	83.13	59.6	23.53

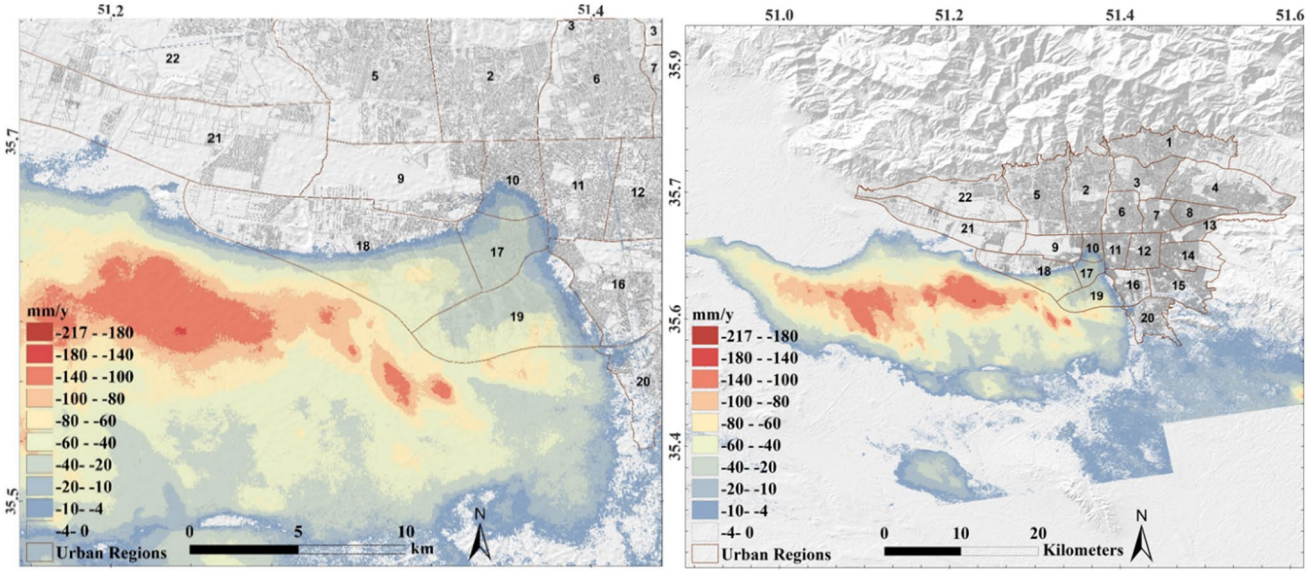

Fig. 7 Districts affected by land subsidence

Fig. 7, the growth of the subsidence zone in the northeastern corner affects the urban district 10 of Tehran at the highest latitude. District 9 is also located on the border of the subsidence zone where Mehrabad Airport is located. The effects of land subsidence on various urban elements in the study area are shown in Fig. 8.

Alluvial fans' landforms, surface drainage, and urban development

In the present study, the elevation zones of Tehran City were divided into three parts. In the northern part of the city, the maximum height is 2200 m. In the second zone, the altitude is between 1250 and 1150. The third zone corresponds to the heights between 1150 and 1050 m, which is considered the southern zone of the city and has a plain situation. Ancient alluvial fans are widely spread in the foothills of the Alborz Mountain range. The height of the ancient alluvial fans varies from 1500 m in northern latitudes to 1150 m in southern latitudes. The young alluvial fans are widely scattered at the bottom and mouth of the valleys, on the ancient alluvial fans. The height of the area where the young alluvial fans are located is between 1100 and 1400 m. There is no appreciable valley in this unit, and only existing waterways, with a general direction from north to south, have affected the topographical changes (Fig. 9). Alluvial plains are widely sponged in young and old alluvial fans. The surface of this unit is generally flat, but it slopes gently to the south. As can be seen from Fig. 9, the northern part of the subsidence zone happens in the area of young alluvial fans. This observation suggests that there might be an association between young alluvial fans and subsidence.

Figure 9 shows that the rivers of the region drain surface runoff from north to south and direct it to the southern plains of Tehran. The drainage is mainly done by the rivers in the east of Tehran. The area of land subsidence in the area of Tehran is located at the end of the part of Kan and Chitgar alluvial fans (Fig. 9). To assess the subsidence phenomenon, one important factor is attention to the river changes over time. As can be seen in the right panel of Fig. 9, the Derkeh, Farahzad, and Hesarak valleys (Table 4) are connected to the Ken River (in the west) by a diversion channel due to urban physical growth. While, the natural path of each of these rivers was towards districts 9 and 10. Canalization and diversion of rivers can affect the feeding regime of the aquifer. Because the bed of the rivers in the studied area has high drainage due to high permeability, if there is no continuous feeding, the groundwater will lose quickly. It seems that this situation has happened along the Derkeh and Farahzad rivers. This can be one major factor for the development of subsidence towards the northern latitudes in District 10. This observation suggests that the investigation of alluvial

Fig. 8 The effects of land subsidence on various urban elements in the study area

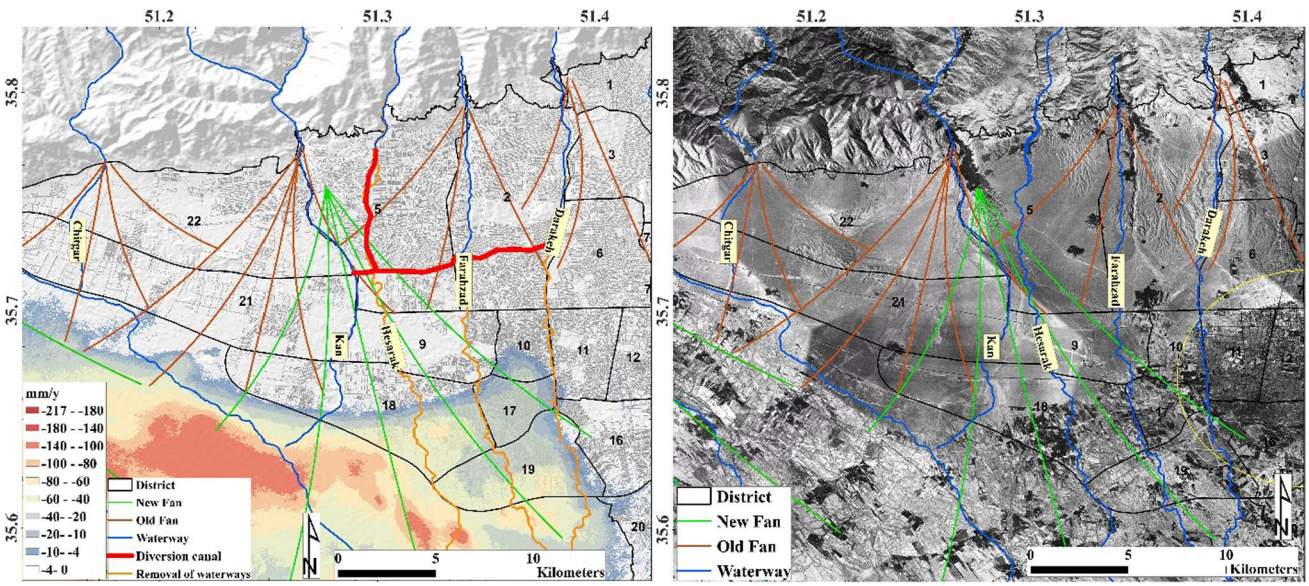

Fig. 9 The verification of the waterways from the old aerial photo on the left side and the diversion channel of Derkeh, Farahzad, and Hesarak waterways to the Ken River, whose extension has been removed over time and in the urban context

fan landforms as well as the alteration of surface drainage patterns is very important in the analysis and evaluation of land subsidence and needs more exploration.

The second step of the surface stage: geomorphology

Figures 10, 11, 12 show the grain size analysis of the northern, middle, and southern zones of Tehran, respectively. In the northern area, the distribution of granulation with sand and coarse particles is predominant (Fig. 10). In this area,

Table 4 Characteristics of important waterways in the western part of Tehran metropolis

Name	Length of the river (km)	Width of the river bed (m)	Moderate slope (%)	Elevation up waterways	Down waterways elevation
Kan	16	35	5	1350	1100
Chitgar	8	10	5.5	1400	1200
Derkeh	18	12	4	1700	1250
Hesarak	8	12	6	1700	1250
Farahzad	13	10	7	1650	1250

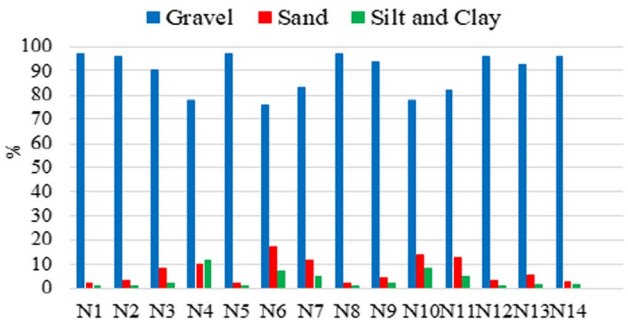

Fig. 10 Grain size analysis in the north of Tehran

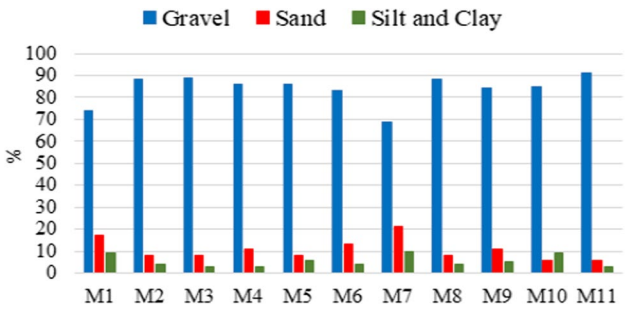

Fig. 11 Grain size analysis in the middle of Tehran

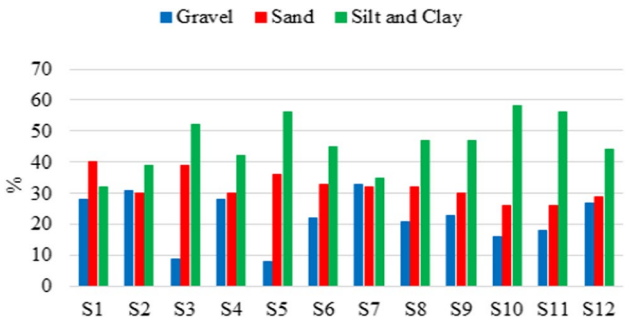

Fig. 12 Grain size analysis in the south of Tehran

in most cases, especially in waterways, the transfer of grains occurs by high mutations and energy with turbulence. The presence of sand lenses among the coarse-grained sediments towards the south indicates a decrease in energy. Sorting is very good in the surface layer sediments, especially in waterways, and medium in the bottom sediments skewing is also towards fine particles. The very large diameter of the particles with very good sorting and mass deposition indicates a very high energy environment in the upper reaches of the northern zone, especially in the rivers. However, the sediments along the rivers with the smaller average diameter and less sorting compared to the layer that is a short distance from the river indicate a decrease in energy in this part (Table 5).

In the middle part (Fig. 11), gravel is dominant, and is distributed with considerable uniformity. The presence of thin layers and in some cases in the form of lenses with sand and mud content indicates turbulence in sedimentation. When the energy is high, coarse-grained gravels are deposited and when the energy is reduced, mud sediments are deposited as a layer and lens. In the middle zone, in most of the layers, there is good sorting and skewing towards small particles. The layers have coarse sediments. In most layers, transport is dominated by traction and some bounce with a very small percentage of suspension. Thin layers and in some cases in the form of lenses, whose content is fine-grained sand, clay, and silt, are present in the layers close to the surface, which indicates the disturbance of the sedimentation. When the energy of the environment is high, coarse-grained sands are deposited, and after the energy decreases, the fine-grained sediments are deposited as thin layers and lenses on the previous coarse-grained sediments (Table 5).

In the southern zone (Fig. 12), the suspended load has low energy and the distribution of fine grains (silt and clay) is dominant. In some cases, there is a thick layer of clay sediments between the coarse grain layers which indicates high fluctuation in water energy and this means that the energy of the environment has alternately increased or decreased. The sedimentation of fine particles indicates a sudden decrease in the speed of water flow. The brick kilns indicate fine-grained sediments in this region. In this area, the grain size becomes coarser from the surface of the earth in the direction of depth (Table 5). This case is more noticeable in the southwestern part of the studied area and in the place that is affected by land subsidence. In Fig. 13A–C, the texture of sediments in

Table 5 Sedimentological studies in the study area

	Sedimentological information of the northern part of the Tehran			Sedimentological information of the middle part of the Tehran			Sedimentological information of the southern part of the Tehran		
	Average	Highest	Lowest	Average	Highest	Lowest	Average	Highest	Lowest
Size	1347.5	2464 microns	231 microns	925.5	1795 microns	56 microns			
Sorting	Bad	Medium	Good@		Microns	Microns	830	1600 microns	60 microns
			@	Bad	Medium@	Good	Bad@	Medium	Good
Width	2.65	3.4	1.9		@		@		
Sphericity	0.53	0.57	0.5	2.7	2.78	1.8	2.19	2.7	1.68
				0.55	0.64	0.46	0.61	0.72	0.51
Average diameter of small grains	40.95 mm	60.8 mm	21.1 mm	29.9 mm	42.4 mm	17.5 mm	29.9 mm	42.3 mm	17.5 mm
Average diameter of medium grains	51.8 mm	72.3 mm	31.3 mm	52.7 mm	74.6 mm	30.97 mm	52.7 mm	74.6 mm	30.97 mm
Average diameter of large grains	92.25 mm	108.9 mm	51.2 mm	84.4 mm	113 mm	55.9 mm	84.9 mm	113 mm	55.9 mm

Fig. 13 Texture of sediments in the northern (**A**), middle (**B**), and southern (**C**) zones of the study area

the northern (A), middle (B), and southern (C) zones have been shown.

Considering Figs. 10, 11, 12, it is obvious that in comparison to the northern and middle zones of Tehran, the ratio of sand and silt is much more than gravel in the southern zone. The soil with sand and silt is much more susceptible to compaction and shrinkage. This observation and the fact that the southwestern zone of Tehran experiences subsidence strengthens the hypothesis that the silt and sand soil type could be an important factor in the formation and development of the subsidence in Tehran city. Therefore, in the sub-surface studie,s soil grading was also investigated.

Results of sub-surface studies

First step of sub-surface studies: groundwater

Figure 14 shows the groundwater level map using piezometric data in 2017, which decreases from north to south. The groundwater level is high in the southwestern areas, which include the areas with the highest amount of land subsidence (urban area 18). In general, the depth of water in Tehran City decreases from west to east and from north to south, and in areas that have subsidence, the groundwater level is distributed at relatively higher depths than in the southeast of Tehran. In general, the thickness of the alluvium is high in the southwestern regions, and with the loss of groundwater, the compressive force in the direction of gravity also increases, which results in compaction and subsidence of the land. The changes in groundwater in 2001 and 2017 (Fig. 15) show that even though the groundwater drop is high in the middle and near the top of

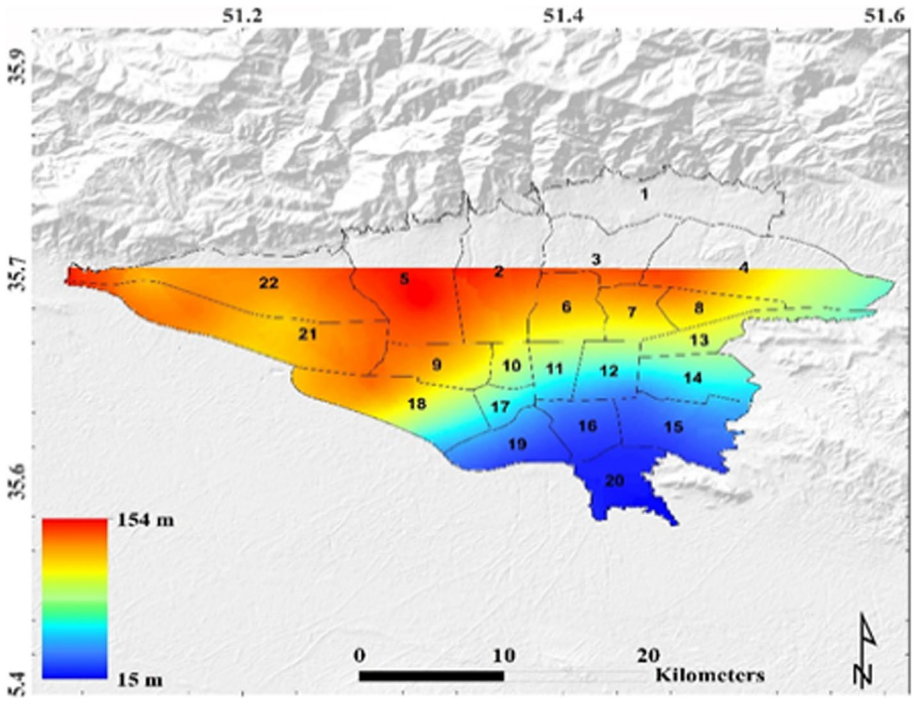

Fig. 14 The water table map of the study area on 2015 data

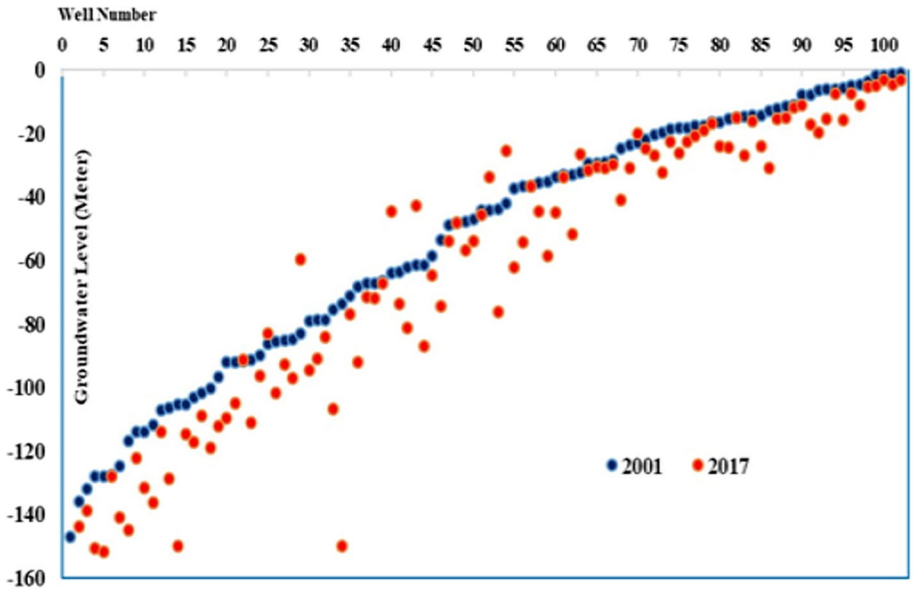

Fig. 15 The ground water changes from 2001 to 2017

the alluvial fan, there is no sign of land subsidence in the form of a zone. This issue is due to the physical characteristics of sediment granulation. However, in the southern latitudes, the occurrence of land subsidence has a direct relationship with the drop in the groundwater level. Similarly, no significant subsidence is observed in the southeastern regions of Tehran. Unlike the southwestern regions, which comprise the alluvial fans of Kan and Chitgar, the southeastern regions of Tehran primarily consist of limestone and volcanic rocks, devoid of alluvial fans. Furthermore, the thickness of the alluvium is smaller in the southeastern area, and this region has experienced a lesser drop in the underground water level.

Second step of sub-surface studies: geotechnical investigation

Distribution of gravel A comparison of gravel distribution maps (Fig. 16) at the studied depths shows major changes in the dominant distribution of gravel in the northeast, northwest, and southwest regions. In the depths of 5 and 10 m in

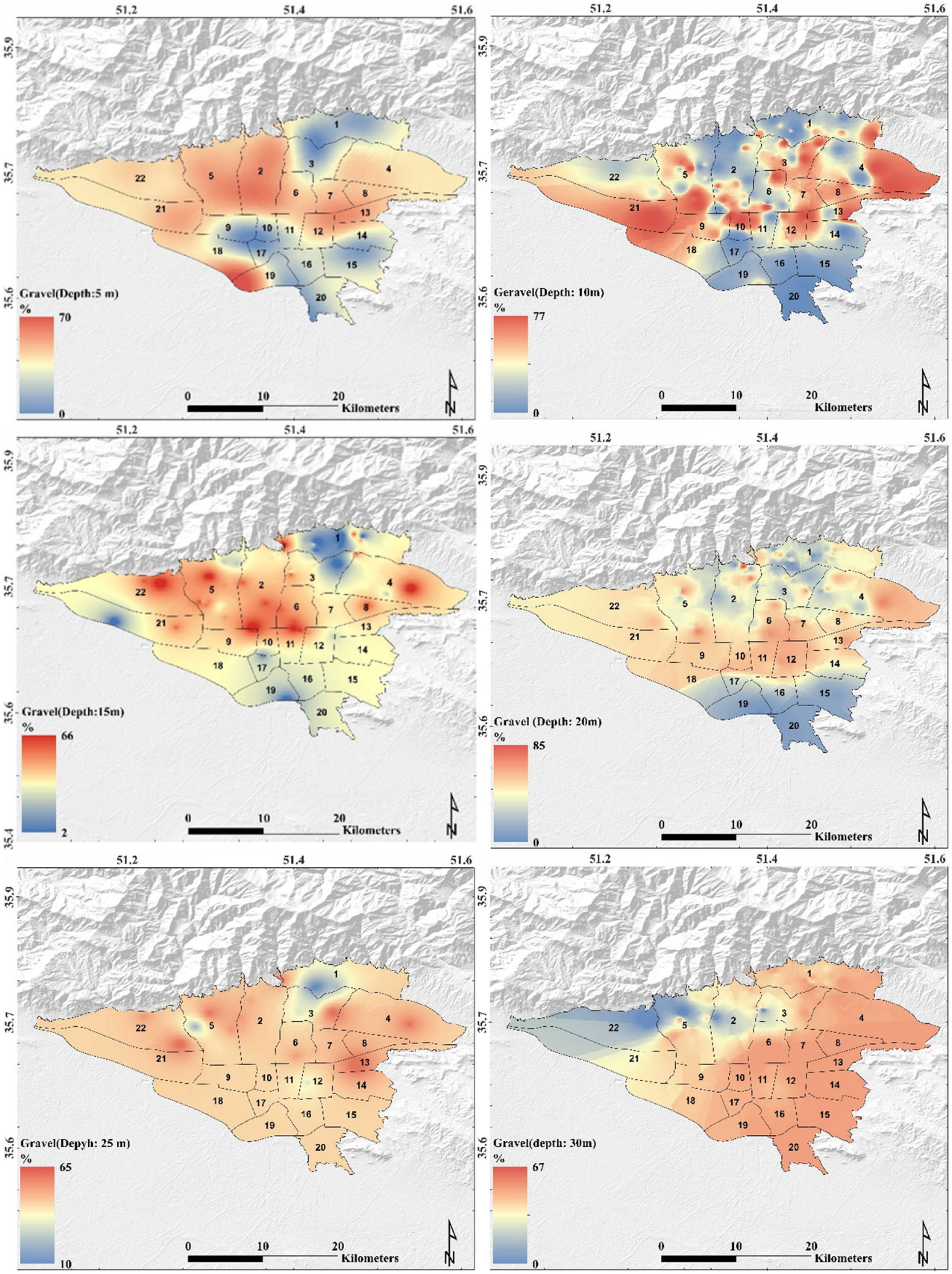

Fig. 16 Gravel distribution map in depths of 5, 10, 15, 20, 25, and 30 m

the northern half, the highest percentage of gravel distribution was obtained. At a depth of 5 m and in urban districts 9 to 11, 16, and 17 and the northwest districts 18 and 19 which are affected by subsidence, the gravel is distributed with a relatively small percentage (less than 20%) that reaches the lowest value at a depth of 10 m. At a depth of 15 m, the percentage of gravel distribution increases in the mentioned districts except for districts 17 and 19. At a depth of 20 m, the distribution of gravel continues in the southern latitudes of districts 9–11, which is different from the previous levels. In fact, in Districts 9–11, as well as in the western half of District 18, the distribution of gravel is around 60%, but in Districts 16, 17, 19, and the eastern half of District 18, the distribution is less than 20%. At the depths of 25 and 30 m, the distribution of gravel increases significantly and reaches more than 50%. The high distribution of gravel in the lower levels indicates water permeability and drainage (Fig. 18).

Distribution of sand The percentage of sand distribution varies from one point to another and also at different depths (Fig. 17), but it follows a relatively moderate level compared to the distribution of gravel and fine grains. The highest percentage of sand is distributed in the middle zone of Tehran. The lowest distribution percentage is related to southern latitudes. The relatively average distribution of sand in the study area can be an effective factor in mixing with fine grains in the rate of infiltration and drainage of the lower surfaces. The pattern of sand distribution is consistent with the results of sedimentology.

Distribution of fine grains The distribution of fine grains in the areas affected by subsidence is very significant and consistent with the subsidence pattern (Fig. 18). The highest percentage of fine grain distribution includes the southern parts of districts 9, 10, and 11 to the latitudes where districts 16–19 are located. In general, the distribution of fine grains in the studied area is inversely related to the distribution of gravel but correlated with the subsidence pattern. The western half of District 18, which has a low percentage of the distribution of fine grain due to the abundance of gravel, is also in the waterways and the Kan alluvial fan. As can be seen in Fig. 9, this part of District 18 has not experienced significant subsidence.

According to the SPT values, this part is high in terms of density and shear strength, and the n number with a maximum value of 320 is proof of this. In the northwest and southeast of the studied area, there are also numbers that show high density (more than 50), but in the southwestern part, this parameter has the lowest value, which is between 20 and 50.

SPT Figure 19 presents the SPT results in Tehran. The figure shows that most parts of Tehran have medium-to-high loading capacity, but the results are different in the areas affected by subsidence. Northeast of the city is located in the area of alluvial formation (Hezar Darreh Geology Unit). According to the SPT values, this part is high in terms of density and shear strength, and the 'n' number with a maximum value of 320 is proof of this. In the northwest and southeast of the studied area, relatively large '*n*' numbers (more than 50) indicate high density. However, in the southwestern part, this parameter has the lowest value, which is between 20 and 50. The sediments of this section are low in terms of density and resistance and react to the compressive force resulting from the drop of groundwater and the subsequent increase in weight. In fact, the bearing capacity and resistance of sediments in these areas are low to very low. Considering Fig. 7, the subsidence zone is consistent with the area of low SPT results. This indicates that the loading capacity of the soil can be an important factor in the formation of subsidence.

Discussion of the results

The study of land subsidence should be comprehensive, and this research has aimed to achieve that. However, the depth of analysis in each step can be enhanced with additional information and data. In this study, the minimum available data was utilized. By considering the results obtained from the evaluation of surface and sub-surface data, the authors suggest the following interpretation for the mechanism of subsidence in Tehran.

The results show that the area of land subsidence in the metropolitan area of Tehran is located in the end part of the alluvial fan of Ken and Chitgar. The changes in flow energy have caused intermittent alluvial fan deposits. The distribution of a significant percentage of gravel in the lower levels, which is related to the young alluvial fan of this region, has high permeability. The high compressibility in the area affected by the subsidence is also related to the young alluvial fans that have spread over the ancient alluvial fans. In the northern latitudes, in the area of alluvial fans, although the drop in the groundwater level is high, it is not affected by the subsidence due to coarse-graining and dense texture. This issue can be related to ancient alluvial fans, but the situation is different in the southern parts. The placement of fine grains with high compressibility on gravelly sediments with high permeability is condensed due to the drop in the groundwater level and leads to land subsidence.

Regarding the drop in the underground water level, there are four cases as the most important factors. The first case is related to the physical growth and development of the city over time, which reduces the penetration of water to the depths below. Also, the demand for water consumption has increased and has led to the use of underground water. Furthermore, the increase of agricultural wells in the west

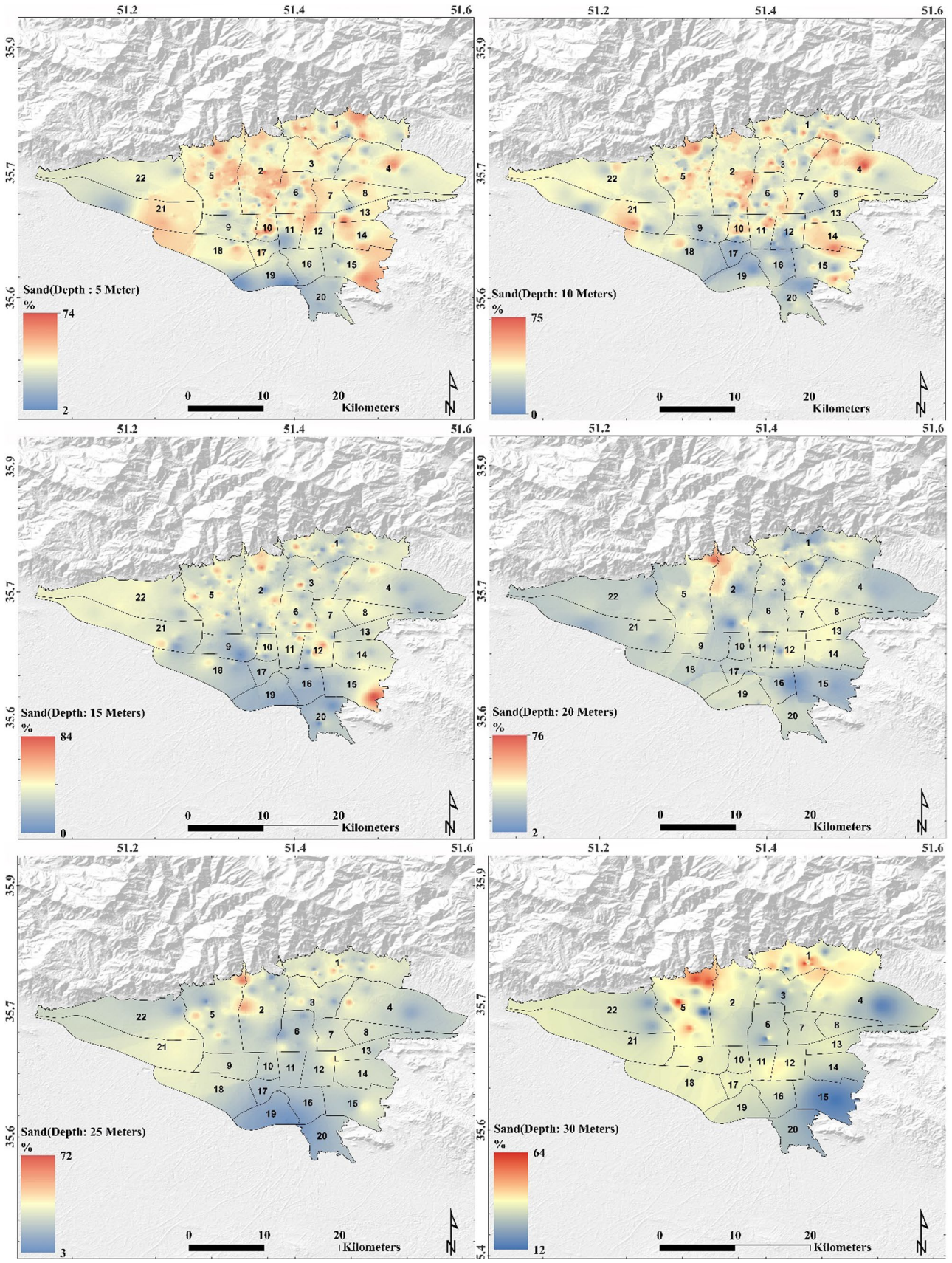

Fig. 17 Sand distribution map in depths of 5, 10, 15, 20, 25, and 30 m

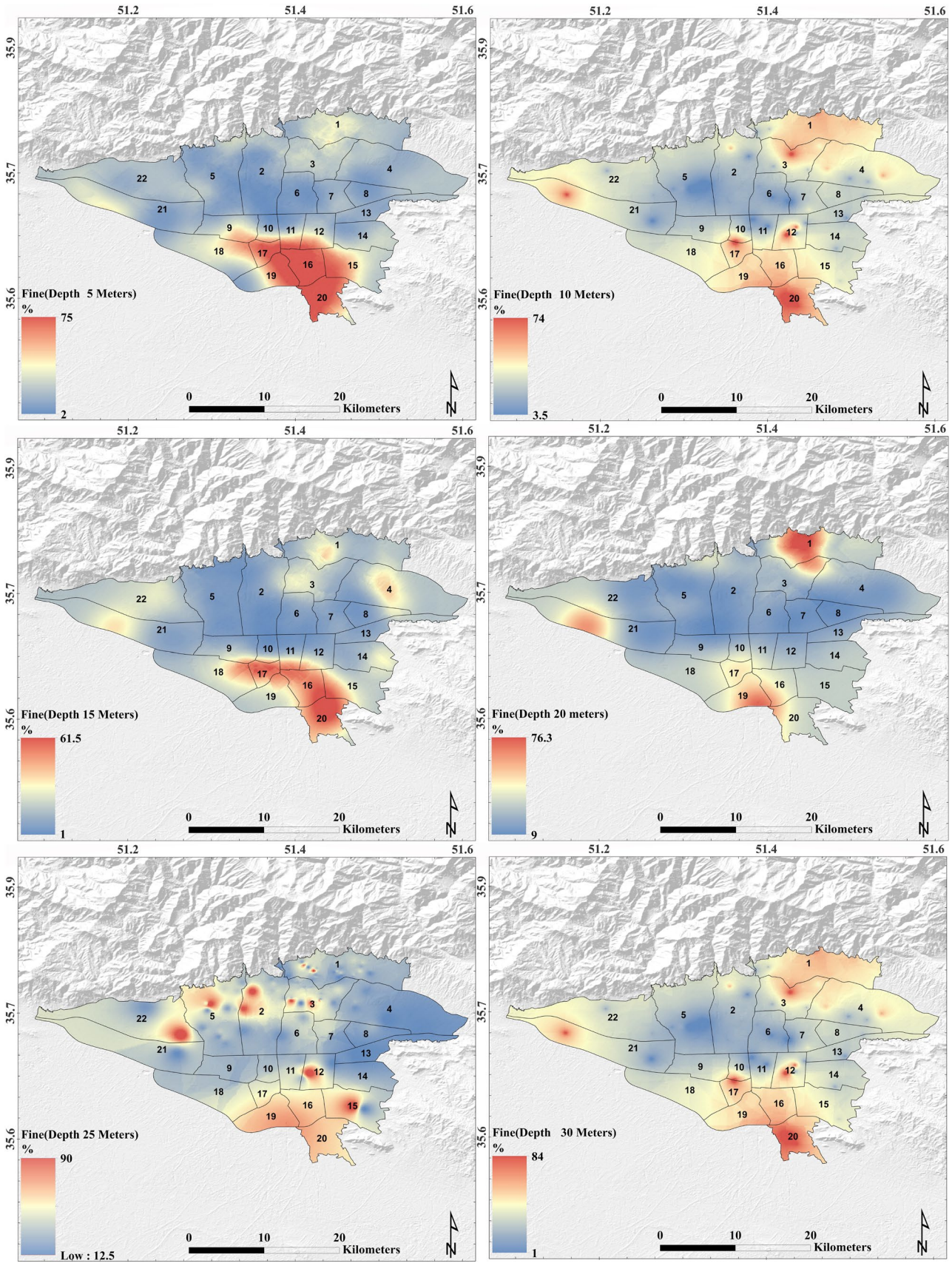

Fig. 18 Fine-grained distribution at depths of 5, 10, 15, 20, 25, and 30 m

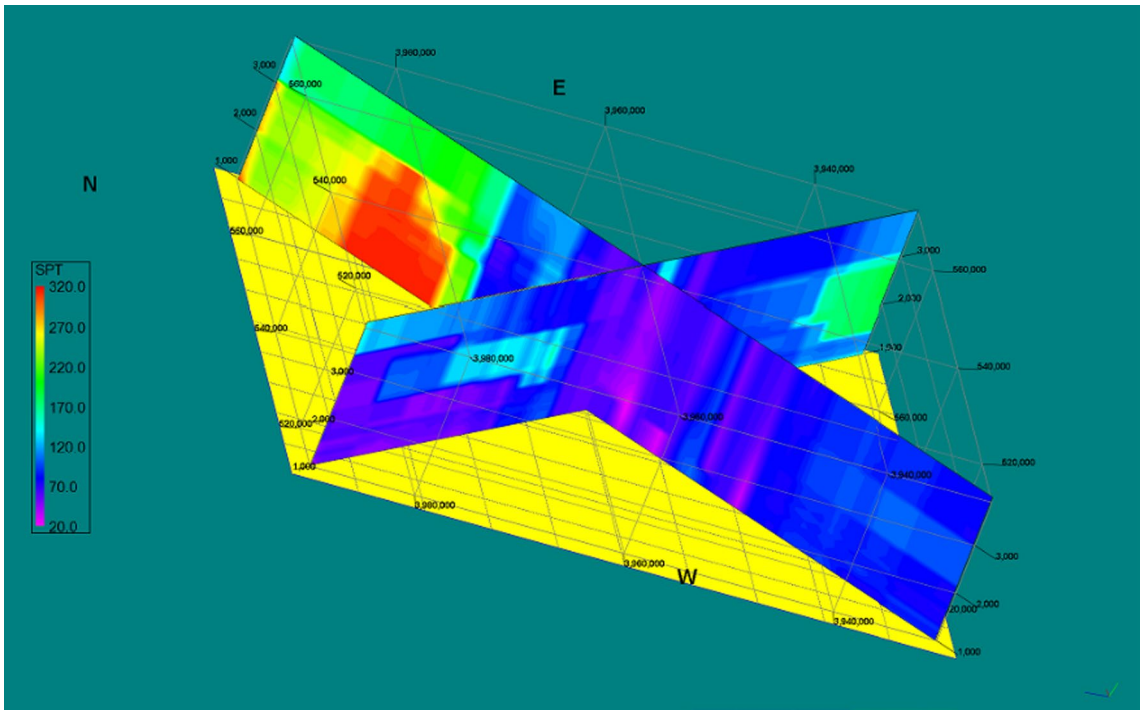

Fig. 19 Density rate (SPT) in the four geographical directions of the study area

of Tehran affects the reduction of the underground water levels. Finally, the diversion of waterways by concrete channels affects the reduction of the groundwater feeding regime. Specially, in District 10, the land subsidence pattern develops towards high latitudes. This area is located next to Derke and Farahzad waterways. With urban development, these waterways have been transferred to the western part and the Ken River by a diversion channel. Because the lower surfaces of the area have a high performance in terms of permeability, due to the change in the direction of these waterways, they are not fed, and with the drop in the groundwater level, it condenses and settles. Unlike the southwestern regions, which comprise the alluvial fans of Kan and Chitgar, the southeastern regions of Tehran primarily consist of limestone and volcanic rocks without alluvial fans. Although the drop in the groundwater level is considerable in this area, no significant subsidence is observed in the southeastern regions. This again, indicates the importance of soil grading and properties in the formation of subsidence.

Urban studies: evaluation of residential density, urban development, and urban decay affected by land subsidence

Figure 20 shows the residential density diagram along with urban decay. It was observed in the field observations that some areas located in the subsidence zone have wide open

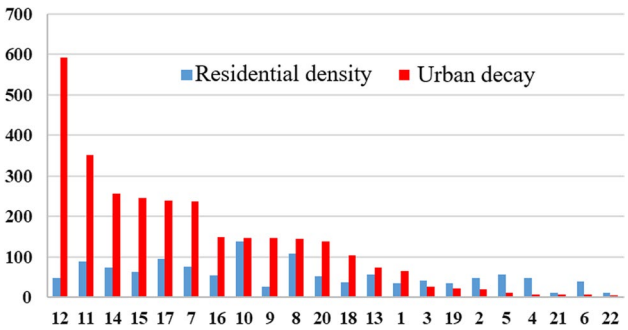

Fig. 20 Residential density statistics in 22 districts of Tehran

spaces (districts 17, 18, and 19 are among these areas). The distribution of residential units in each of these areas is not uniform and these regions consist of two parts, open space, and residential space. If the open areas are removed, the residential density and building density (Fig. 21) will increase significantly. In relation to the urban decay (Fig. 22), districts 11 and 12 (the oldest region and initial core of Tehran city) have the most decay among the urban areas. Districts 17, 10, 18, and 19 are in the next ranks, respectively, which are affected by subsidence. Meanwhile, the entire district of 17 is located in the subsidence zone, which has a high rank in terms of urban decay.

Fig. 21 Pictures of building density in the districts with subsidence

Fig. 22 Images of the urban decay in the study area

In the field visits, it was observed that in addition to the residential building, other important elements are also affected by the subsidence of the earth, which will lead to unfortunate events if secondary phenomena, such as sinkholes and deep cracks, occur. Railway lines, highways, and bridges were among the elements that were observed during the field visits, which showed traces of cracks and displacements that were probably due to the subsidence of the earth. In this regard, the Azadegan highway is one of the most important transportation axes in the southern edge of Tehran, Shahid Kazemi, and Ayatollah Saeedi highways in the 17th, 18th, and 19th districts, Shahid Tandgoyan highway in the 19th district, and Shahid Rajaei highway can be mentioned. They are in charge of transportation in and out of the Tehran metropolis. During the field visits, more than 25 bridges were observed and identified in the area of land subsidence with high risk. There are also about 20 bridges on the edge of the subsidence zone. All bridges are located on highways and main thoroughfares. Tehran's metropolis as the capital of the country has high sensitivity in relation to land subsidence.

In the area of Tehran's metropolis, the following actions need to be taken: preventing the drilling of new wells, installing meters, and limiting the water consumption of wells that are being used for agricultural purposes. Monitoring the type of cultivation and preventing the cultivation of water-intensive crops. Feeding the underground water table (e.g., by reviving the main course of waterways and directing surface flows to them during rains), permanent monitoring of the ground subsidence phenomenon, and studying the bedrock of the area and the thickness of the alluvium to study and estimate the maximum land subsidence. Determining the construction code with an emphasis on the ground subsidence phenomenon and subsidence risk should be done for all urban elements.

Conclusions

This study provides a comprehensive investigation of surface and sub-surface factors that affect subsidence and investigates the mechanism of subsidence development in Tehran. Land surface studies involve assessing the subsidence rate and pattern by utilizing InSAR technology, tracking the urban development of the city, and investigating geomorphological features like the alluvial fans landforms and surface drainage. Sub-surface studies include groundwater and geotechnical assessments and reveal the role of each of them on subsidence. In addition, residential density and dilapidated fabric were investigated as the most important examples of risky urban elements exposed to the phenomenon of land subsidence.

The results of the radar interferometric study in the present study had two important results. The first result was the amount of ground subsidence and the second was its pattern. The results show that the amount of ground subsidence was highly underestimated in some previous studies (e.g., from 11.5 mm per year to 36 mm per year). In this study, the maximum amount of land subsidence was 217 mm per year in the southwest. Land subsidence was obtained in an area with a width of about 700 km. An important result of this stage was the northward development of the land subsidence zone in the northeastern corner (which indicates a direct development of the subsidence zone in the urban areas). The development of Tehran over time has caused many changes in alluvial cone landforms and waterways. As it was observed, as a result of the physical development of the city, the canals of Hesarak, Farahzad, and Derkeh have been directed to the west and the Ken River by a concrete channel. While these waterways have flowed in the past with their natural course in the general north–south direction. Also, geotechnical studies showed that with increasing depth, the amount of gravel and coarse grains distribution increases, which shows high permeability in urban areas and corresponds to the middle and lower latitudes of unconsolidated and young alluvial cones of Chitgar, Ken, and Farahzad. The diversion of waterways, the high permeability of sediments in the depths below, the consolidation of non-solidification, high compressibility, and the drop in the underground water level were the main factors that led to the phenomenon of land subsidence.

Examining the housing density and worn-out fabric of urban areas affected by land subsidence showed that these areas are not in good condition, and in case of secondary phenomena such as subsidence, sinkholes, and cracks, it can cause a lot of damage. Other important elements, such as communication arteries and infrastructures, will be damaged if the mentioned phenomena occur.

Author contributions AM: conceptualization, methodology, writing original draft, collecting the necessary data and processing, formal analysis, review, and editing. SE: conceptualization, methodology, writing original draft, formal analysis, review, and editing. HA: participation in writing original draft, formal analysis, review, and editing. BG: analysis in geotechnical data and writing original draft.

Funding No funds, grants, or other supports were received.

Availability of data and materials The datasets used during and/or analyzed during the current study are available from the corresponding author upon reasonable request.

Declarations

Conflict of interest The authors declare that they have no known competing financial interests or personal relationships that could have appeared to influence the work reported in this paper.

Ethics approval Not applicable.

Consent to participate Informed consent was obtained from all individual participants included in the study.

Consent to publish All the authors permit the Publisher of the authors to publish the research work.

Consent for publication The authors agree to publish this article in the Environmental Earth Sciences.

References

Amighpey M, Arabi S, Talebi A, Djamour Y (2006) Elevation changes of the precise leveling tracks in the Iran leveling network. In: Scientific report published in National Cartographic Center (NCC) of Iran (in Persian)

Berardino P, Fornaro G, Lanari R, Sansosti E (2002) A new algorithm for surface deformation monitoring based on small baseline differential SAR interferograms. IEEE Trans Geosci Rem Sens 40:2375–2383. https://doi.org/10.1109/TGRS.2002.803792

Chatrsimab Z, Alesheikh A, Vosoghi B, Behzadi S, Modiri M (2020) Land Subsidence modelling using particle swarm optimization algorithm and differential interferometry synthetic aperture radar. Ecopersia 8:77–87

Chaussard E (2016) Subsidence in the Parícutin lava field: Causes and implications for interpretation of deformation fields at volcanoes. J Volcanol Geotherm Res 320:1–11. https://doi.org/10.1016/j.jvolgeores.2016.04.009

Dang VK, Doubre C, Weber C, Gourmelen N, Masson F (2014) Recent land subsidence caused by the rapid urban development in the Hanoi region (Vietnam) using ALOS InSAR data. Nat Haz Earth Syst Sci 14:657–674. https://doi.org/10.5194/nhess-14-657-2014

Dehghani M, Valadan Zoej MJ, Hooper A, Hanssen RF, Entezam I, Saatchi S (2013) Hybrid conventional and persistent scatterer SAR interferometry for land subsidence monitoring in the Tehran Basin Iran. ISPRS J Photogramm Remote Sens 79:157–170. https://doi.org/10.1016/j.isprsjprs.2013.02.012

Dobkins JE, Folk RL (1970) Shape development on Tahiti-Nui. J Sediment Petrol 40:1167–1203

Esmaeili M, Motagh M (2016) Improved Persistent Scatterer analysis using Amplitude Dispersion Index optimization of dual polarimetry data. ISPRS J Photogramm Remote Sens 117:108–114. https://doi.org/10.1016/j.isprsjprs.2016.03.018

Esmaeili M, Motagh M, Hooper A (2017) Application of dual-polarimetry SAR images in multiemporal InSAR processing. IEEE Geosci Remote Sens Lett 14:1489–1493. https://doi.org/10.1109/LGRS.2017.2717846

Galloway DL, Burbey TJ (2011) Review: Regional land subsidence accompanying groundwater extraction. Hydrogeol J 19:1459–1486. https://doi.org/10.1007/S10040-011-0775-5

Ge L, Chang HC, Rizos C (2007) Mine subsidence monitoring using multi-source satellite SAR images. Photogramm Eng Remote Sens 73:259–266

Goorabi A, Karimi M, Yamani M, Perissin D (2020) Land subsidence in Isfahan metropolitan and its relationship with geological and geomorphological settings revealed by Sentinel-1A InSAR observations. J Arid Environ. https://doi.org/10.1016/j.jaridenv.2020.104238

Haghshenas Haghighi M, Motagh M (2019) Ground surface response to continuous compaction of aquifer system in Tehran, Iran: Results from a long-term multi-sensor InSAR analysis. Remote Sens Environ 221:534–550. https://doi.org/10.1016/j.rse.2018.11.003

Karami E, Alizadeh N, Farhadi H, Abdolazimi H, Maghsoudi Y (2023) Monitoring of land surface displacement based on InSAR-time-series and GIS techiques: a case study over the Shiraz Metropolis, IRAN, Int. Arch Photogramm Remote Sens Spat Inf Sci 4:371–378. https://doi.org/10.5194/isprs-annals-X-4-W1-2022-371-2023

Kooi H, De Vries JJ (1998) Land subsidence and hydrodynamic compaction of sedimentary basins. ydrol. Earth Syst Sci 2:159–171. https://doi.org/10.5194/hess-2-159-1998

Li Z, Chen Q, Xue Y, Qiu D, Chen H, Kong F (2023a) Numerical investigation of processes, features, and control of land subsidence caused by groundwater extraction and coal mining: a case study from eastern China. Environ Earth Sci. https://doi.org/10.1007/s12665-023-10779-5

Li J, Smith R, Grote K (2023b) Analyzing spatio-temporal mechanisms of land subsidence in the Parowan Valley, Utah, USA. Hydrogeol J 31:1–9. https://doi.org/10.1007/s10040-022-02583-5

Mahmoudpour M, Khamehchiyan M, Nikudel MR, Ghassemi MR (2016) Numerical ssimulation and prediction of regional land subsidence caused by groundwater exploitation in the southwest plain of Tehran. Iran Eng Geol 201:6–28. https://doi.org/10.1016/j.enggeo.2015.12.004

Motagh M, Walter TR, Sharifi MA, Fielding E, Schenk A, Anderssohn J, Zschau J (2008) Land subsidence in Iran caused by widespread water reservoir overexploitation. Geophys Res Lett. https://doi.org/10.1029/2008GL033814

Nyakundi R, Nyadawa M, Mwangi J (2022) Effect of recharge and abstraction on groundwater levels. J Civ Eng 8:910–925. https://doi.org/10.28991/CEJ-2022-08-05-05

Pirouzi A, Eslami A (2017) Ground subsidence in plains around Tehran: site survey, records compilation and analysis. Int J Geo-Eng 8:30. https://doi.org/10.1186/s40703-017-0069-4

Pishro M, Khosravi S, Tehrani SM, Mousavi SR (2016) Modeling and zoning of land subsidence in the southwest of Tehran using artificial neural networks. Int J Hum Cap Urban Manag 1:159–168. https://doi.org/10.22034/ijhcum.2016.03.002

Rajabi Baniani S, Chang L, Maghsoudi Y (2021) Mapping and analyzing land subsidence for Tehran using Sentinel-1 SAR and GPS and geological data. In EGU Gen Assem Conf Abstr. https://doi.org/10.5194/egusphere-egu21

Ranjbar A, Ehteshami M (2019) Development of an uncertainty based model to predict land subsidence caused by groundwater extraction (case study: Tehran Basin). Geotech Geol Eng 37:3205–3219. https://doi.org/10.1007/s10706-019-00837-w

Rodriguez JM, Edeskär T, Knutsson S (2013) Particle shape quantities and measurement techniques—a review. Electron J Geotech Eng 18:169

Shennan I, Hamilton S (2006) Coseismic and pre-seismic subsidence associated with great earthquakes in Alaska. Quat Sci Rev 25:1–8. https://doi.org/10.1016/j.quascirev.2005.09.002

Sneed M, Ikehara ME, Stork SV, Amelung F, Galloway DL (2003) Detection and measurement of land subsidence using interferometric synthetic aperture radar and global positioning system, San Bernardino County, Mojave Desert, California, U.S. Geol Surv Water Res Investig Rep 3:60. https://doi.org/10.3133/wri034015

Strozzi T, Luckman A, Murray T, Wegmüller U, Werner CL (2002) Glacier motion estimation using SAR offset-tracking procedures. EEE Trans Geosci Remote Sens 40:2384–2391. https://doi.org/10.1109/TGRS.2002.805079

Sun H, Grandstaff D, Shagam R (1999) Land subsidence due to groundwater with drawal: potential damage of subsidence and sea level rise in southern New Jersey, USA. Econ Environ Geol 37:290–296. https://doi.org/10.1007/s002540050386

Teatini P, Ferronato M, Gambolati G, Gonella M (2006) Groundwater pumping and land subsidence in the Emilia–Romagna coastland, Italy: modeling the past occurrence and the future trend. Water Resour Res 42:1–19. https://doi.org/10.1029/2005WR004242

Yesilmaden HM, Inan C, Kurtulus B, Can Canoğlu M, Avsar Ö (2021) Land subsidence assessment under excessive groundwater pumping using ESA Sentinel-1 satellite data: a case study of Konya Basin, Turkey. Environ Earth Sci 80:409. https://doi.org/10.1007/s12665-021-09718-z

Yousefi R, Talebbeydokhti N (2021) Subsidence monitoring by integration of time series analysis from different SAR images and impact assessment of stress and aquitard thickness on subsidence in Tehran. Iran Environ Earth Sci 80:418. https://doi.org/10.1007/s12665-021-09714-3

Zidane A, Zechner E, Huggenberger P, Younes A (2014) Simulation of rock salt dissolution and its impact on land subsidence. Hydrol Earth Syst Sci 18:2177–2189. https://doi.org/10.5194/hess-18-2177-2014